Structural model of the Au-induced Si(553) surface: Double Au rows

Mariusz Krawiec*
Institute of Physics, M. Curie-Skłodowska University, Pl. M. Curie-Skłodowskiej 1, 20-031 Lublin, Poland
(Received 26 October 2009; revised manuscript received 24 February 2010; published 19 March 2010)

A structural model of Au induced Si(553) surface is proposed. The model is based on the recently revised value of Au coverage of 0.48 monolayers, which suggests the formation of two gold chains on each Si(553) terrace. The resulting structural model, such as the models of other vicinal Si surfaces, features the honey-comb chain, but no buckling of the step edge is observed, unlike in the case of the Si(335)-Au and Si(557)-Au surfaces. The present model is more stable than the models with single Au chain only, and agrees well with existing experimental data. In particular, calculated band structure, featuring two metallic bands coming from the hybridization of gold in both chains with neighboring Si atoms, matches well the photoemission data. Moreover, theoretical scanning tunneling microscopy topographs remain in good agreement with the experiment.

DOI: 10.1103/PhysRevB.81.115436 PACS number(s): 73.20.At, 71.15.Mb, 79.60.Jv, 68.35.B−

I. INTRODUCTION

More than decade ago it has been discovered that submonolayer coverage of gold stabilizes the stepped silicon surfaces, leading to one-dimensional ordering of the surface.[1] Since then various stepped Si surfaces have been extensively studied in relation to expected exotic phenomena, characteristic for the systems of reduced dimensionality.[2,3] Perhaps one of the most known examples is a gold decorated Si(553) surface. The Si(553)-Au surface consists of Si(111) terraces $4\frac{1}{3}\times a_{[11\bar{2}]}=1.48$ nm wide and single atomic steps. The Si(553) surface normal is tilted from [111] direction toward $[11\bar{2}]$ by 12.5°.[4] The properties of this surface have been investigated by number of techniques, including scanning tunneling microscopy (STM),[4–12] angle resolved photoemission (ARPES),[4,5,7,10,13,14] x-ray diffraction,[15–17] and density-functional theory (DFT).[4,18–20]

Topography of the surface, as measured by STM, features single few nanometers long chains on each terrace, which have been identified as originating from the step edge Si atoms. Those chains are observed to have 3.84 Å periodicity along the chains, i.e., in $[1\bar{1}0]$ direction, which perfectly matches the Si-Si distance in this direction $a_{[1\bar{1}0]}$. This is completely different from what is observed on other vicinal Si surfaces, such as Si(335)-Au[4,21] or Si(557)-Au,[4,22,23] where chains show periodicity doubling, i.e., STM topography shows maxima along the chains with a period of $2\times a_{[1\bar{1}0]}$. The periodicity doubling on the Si(557)-Au and Si(335)-Au surfaces has been explained in terms of the buckling of the step edge Si atoms,[24,25] according to which every second step edge Si atom occupies the up (down) position. On the Si(553)-Au surface one occasionally observes the periodicity doubling and even oscillations of the topography with a period of $3\times a_{[1\bar{1}0]}$,[8] but this has its origin in defects.[11,12] In general, the observed chains on the Si(553)-Au surface have the periodicity equal to the $a_{[1\bar{1}0]}$.

The photoemission spectrum of the Si(553)-Au surface is dominated by two one-dimensional bands (S_{12} and S_3) with parabolic dispersion.[4,5,7,13] Those bands cross the Fermi energy E_F at different $k_{\|}$, i.e., at 1.18–1.22 (1.25–1.30) 1/Å, and at 1.04 (1.07) 1/Å.[5,7,26] The S_{12} band is split by 85 meV, and the splitting has been identified to be a spin splitting induced by the Rashba spin-orbit (SO) interaction.[13] Similar doublet of the proximal bands is also observed in the case of the Si(557)-Au surface,[27] which is also spin split due to the SO interaction.[28] The origin of the SO split S_{12} band comes from the hybridization of the row of Au with the neighboring Si atoms on the Si(557) terrace. Therefore it is also expected that, in the case of the Si(553)-Au surface, the situation will be similar. The S_3 band observed in the photoemission seems to not suffer from the SO interaction (the SO is very weak) and is very similar to the band observed in the case of the Si(335)-Au surface,[4] which also comes from the hybridization of the Au row with the neighboring Si atoms.[29] Both observed bands have been identified in two models (f2 and p2*) of the Si(553)-Au surface proposed in Ref. 20 (see Fig. 8 of Ref. 20). In the case of the f2 model, we have two bands with similar dispersions like in the photoemission experiments. The S_{12} band comes from the hybridization of the Au row with the neighboring Si atoms, and the S_3 band comes from the unsaturated Si bonds on the surface. However, unlike in the experiment, the SO splitting is of equal magnitude in both bands. On the other hand, the agreement of the band structure calculated for the p2* model with the experimental data is slightly better, i.e., both bands have similar dispersions but the SO splitting is stronger in the lower band. However, the band appearing at higher energies also features some degree of splitting.

Early experimental and theoretical investigations assumed Au coverage to be 0.24 ML, which is sufficient to form a single row of Au atoms per terrace.[4–14,16–18,20] However, recently determined Au coverage on the Si(553) surface is 0.48 ML, i.e., two Au chains per terrace.[30] Thus it is interesting to see if the models based on the revised Au coverage perform better in reproducing the photoemission spectra. In fact two Au chains per terrace are consistent with the experimentally obtained coverage from the x-ray diffraction.[15] However, the calculated band structure for the structural model deduced from this experiment does not agree with the measured photoemission spectra.[19] A widely used coverage of single Au chain for Si(553) surface traces back to the initial assumption of 2/3 ML coverage for Si(111)$\sqrt{3}\times\sqrt{3}$-Au and to 0.44 ML

for Si(111)5×2-Au reconstructions.[31,32] Thus, in light of this new value of Au coverage, most of structural models of the Si(553)-Au surface need to be revised in order to take into account two gold chains per terrace.

The purpose of the present work is to determine a structural model of the Si(553)-Au surface, which accommodates two gold chains, and calculate corresponding band structure. The structural model derived from first principles density functional calculations features two Au rows running parallel to the step edges and located in the middle of terraces. The step edge Si atoms rebond in order to form a honey-comb (HC) structure, which is also present on other vicinal Si surfaces.[4,29] This structural model is more stable than other structural models with single Au chain[18,20] and the model deduced from the x-ray diffraction.[15] Moreover, the calculated band structure for this model matches well the measured ARPES spectra, showing two metallic bands associated with the hybridizing Au rows with the neighboring Si atoms. The rest of the paper is organized as follows. In Sec. II, the details of calculations are provided. The structural models of Si(553)-Au surface are presented and discussed in Sec. III, while Secs. IV and V are devoted to the simulated STM topography images and the electronic band structure, respectively. Finally, Sec. VI contains some conclusions.

II. DETAILS OF CALCULATIONS

The calculations have been performed using standard pseudopotential density functional theory and linear combination of numerical atomic orbitals as a basis set, as implemented in the SIESTA code.[33–37] The local density approximation (LDA) to DFT,[38] and Troullier-Martins norm-conserving pseudopotentials[39] have been used. In the case of Au pseudopotential, the semicore 5*d* states and the scalar relativistic corrections were included. A double-ζ polarized (DZP) basis set was used for all the atomic species.[34,35] The radii of the orbitals for different species were following (in a.u.): Au-7.20 (5*d*), 6.50 (6*s*) and 5.85 (6*p*), Si-7.96 (3*s*), 7.98 (3*p*) and 4.49 (3*d*), and H-7.55 (1*s*) and 2.94 (2*p*). A Brillouin zone sampling of 12 nonequivalent *k* points, and a real-space grid equivalent to a plane-wave cutoff 100 Ry have been employed.

The Si(553)-Au system has been modeled by four silicon double layers and a vacuum region of 19 Å. All the atomic positions were relaxed until the maximum force in any direction was less than 0.04 eV/Å, except the bottom layer. The Si atoms in the bottom layer were fixed at their bulk ideal positions and saturated with hydrogen. To avoid artificial stresses, the lattice constant of Si was fixed at the calculated value, 5.39 Å.

III. STRUCTURAL MODELS

Searching for the lowest energy structural model of any surface is an uphill task. There are some sophisticated methods, like genetic algorithms,[40–43] that can find optimal geometries of the system. Those methods are computationally very expensive and are mostly restricted to the use of empirical interatomic potentials, which requires to check the most stable structures using *ab initio* methods. The genetic algorithms have been successfully applied to study the Si(114),[40,42] Si(337)[41] and Si(103)[43] surfaces. However, in the case of the Si(553)-Au surface we deal with Si and Au atoms, and there are no reliable empirical potentials to represent the interaction between the Si and Au atoms. Therefore, one usually adapt a common DFT-based approach, in which one generates some trial configurations and compares the total energies of the resulted structures. This heuristic approach does not guarantee that the lowest energy configuration corresponds to the global energy minimum. However, one can hope to end up in the global minimum, if the resulted atomic configuration is supported by some physical arguments. Recently, a DFT-based method of an exhaustive search of the structural models has been proposed.[20] The idea of this method is to automatically generate trial geometries and iteratively step-by-step increase the accuracy and the computational cost of the calculations. A compact notation has been developed, in which different surface topologies are mapped into a string of numbers. This allows for the enumeration and systematic computation of the structures.

In the case of the vicinal Si surfaces it was shown that it is energetically favorable for the Au atoms to substitute into the top Si layer.[4,24,29] The surface energy gain per unit cell is more than 1 eV, as compared to the adsorption of Au. Therefore, in the following, I will focus on some structural models of the Si(553)-Au surface featuring the substitution of some of the top Si layer atoms by gold.

A. Models with the ×1 periodicity

Since the STM measurements[4–12] show that the topography modulation along the chains is equal to the Si-Si distance in direction $[1\bar{1}0]$, it is natural to take for calculations a single unit cell in this direction (see Fig. 1). This can be also supported by the fact that the buckling is not observed on the Si(553)-Au surface, in contrast to the Si(557)-Au and Si(335)-Au surfaces.[24,25]

Almost all the proposed structural models of the Si(553)-Au surface[4,18,20] feature a single Au chain per terrace, as the determined Au coverage was twice as small as the actual one.[30] Only the model, accounting for two Au chains, was deduced from the x-ray diffraction experiment,[15] and further verified by the DFT calculations.[19] According to that model, the Au atoms adsorb near the Si step edges. However, none of the proposed structural models managed to reproduce the phootemission spectra. The present investigations of the structural models of the Si(553)-Au surface with proper Au coverage (2 Au atoms per the Si(553) surface unit cell) show that the more stable models feature the Au atoms substituted for the top Si layer atoms in the middle of terrace.

Figure 1 shows the most stable structural model (m1) of the Si(553)-Au surface, where the Si surface atoms (Si_1-Si_7) are labeled by numbers 1–6 and two gold atoms by Au_1 and Au_2. This model is energetically more favorable than the most stable Si(553)-Au model with a single Au row (f2 model of Ref. 20) for the relative chemical potential of Au $\Delta\mu_{Au}=\mu_{Au}-\mu_{Au}^{bulk}$ down to −1.65 eV, and the calculated surface energy is 12.40 meV/Å^2 lower in the Au-rich limit.[44] In

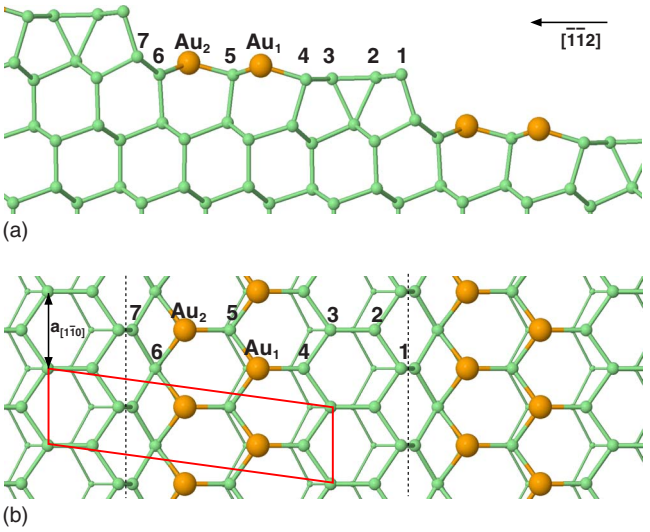

FIG. 1. (Color online) Structural model (m1) of the Si(553)-Au surface. Top panel shows side view of the structure, and bottom panel shows top view with marked surface unit cell and Si-Si distance in the $[1\bar{1}0]$ direction ($a_{[1\bar{1}0]}$). The second uppermost Si double layer is also shown in the bottom panel. Labels 1–7 stand for the silicon surface atoms (Si_1-Si_7), while Au_1 and Au_2 denote the gold atoms. The dashed lines in the bottom panel indicate the step edges.

fact, the present model is similar to the f7 model of Ref. 20. Replacing one additional silicon atom in that model with the gold (Au_1) results in the structural model shown in Fig. 1. Some of the other models, in which Au atoms occupy various top layer Si positions, shown in Fig. 2, have slightly higher energies. The differences are usually in the range of a few meV/Å^2, and the next "best" structural model (m2) has energy only 3.49 meV/Å^2 higher. The surface energies of the most stable (out of 36 models studied) structural models referred to the most stable model with single Au row (f2 model of Ref. 20), are summarized in Table I.

Although the energy differences between various models listed in Table I are rather small, there are other arguments supporting the model shown in Fig. 1. First one is that the model has the lowest surface energy. Second one concerns the HC chain. It is widely accepted that the structural models of Au decorated vicinal Si surfaces should posses the honeycomb chain at the step edges. The main feature of HC structure is the presence of a true double bond between Si_2 and Si_3 atoms (see Fig. 1), which is responsible for stability of the HC chain.[45] However, other models with the HC chain at the step edge have much higher energies (compare m7, m9 and m4 models shown in Fig. 2). Third argument, concerning the band structure, also supports the present most stable model. The calculated band structure reproduces the photoemission spectra of Refs. 4, 5, 7, and 13 reasonably well. The other models, which have slightly higher the relative surface energies disagree with the ARPES spectra. In particular they do not give correct behavior of the bands near the Fermi energy.

It is known that the other Au decorated vicinal Si surfaces, such as the Si(557)-Au or Si(335)-Au, show the buckling of the step edge Si atoms.[24,25] This manifests itself in the

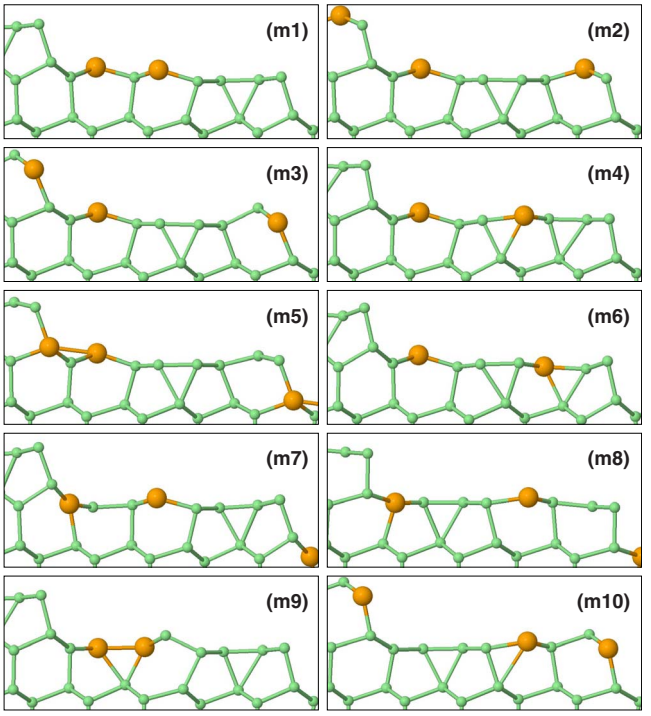

FIG. 2. (Color online) Final geometries of the most stable configurations listed in Table I. Large filled circles denote the Au atoms.

STM topography images as a periodicity doubling along the chains. Since the periodicity of the slab in the $[1\bar{1}0]$ direction taken for calculations is equal to the Si-Si distance in this direction, all the models discussed above do not take into account the possibility of the buckling of the step edge, by definition. This is consistent with the experimental observations.[4–12] However, it is interesting to check if the doubling of the unit cell in the $[1\bar{1}0]$ direction will leave the present model of the Si(553)- Au surface unchanged.

TABLE I. The relative surface energies of the most stable structural models of the Si(553)-Au structure, shown in Fig. 2 (column 2) and their ×2 counterparts (column 3). All the energies are referred to the most stable ×1 model with a single Au row (f2 model of Ref. 20).

Model	×1 Models ΔE (meV/Å^2)	×2 Models ΔE (meV/Å^2)
m1	−12.40	−26.07
m2	−8.91	−8.98
m3	−8.18	−8.18
m4	−6.16	−6.32
m5	−6.16	−6.16
m6	−1.39	−1.39
m7	−0.11	−0.26
m8	−0.11	−0.13
m9	0.63	−9.27
m10	0.63	−1.15

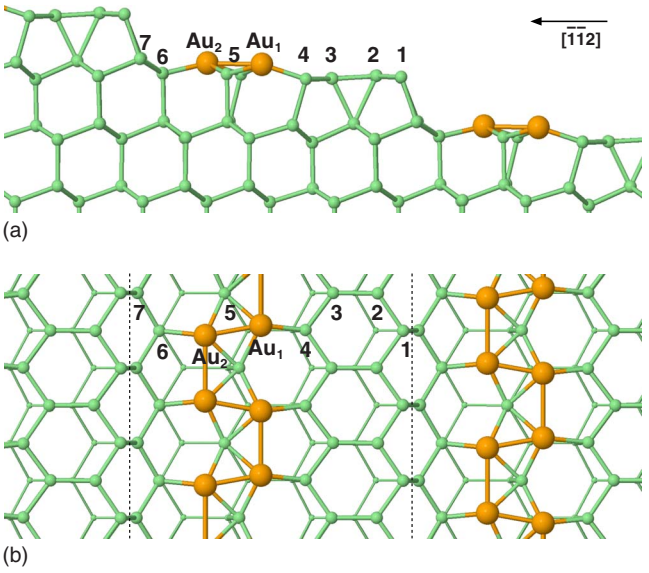

FIG. 3. (Color online) The most stable $\times 2$ structural model of the Si(553)-Au surface. Top (bottom) panel shows side (top) view of the structure. Again, labels 1–7 stand for silicon surface atoms (Si_1-Si_7), while Au_1 and Au_2 denote gold atoms.

B. Models with the $\times 2$ periodicity

Doubling the unit cell along the step edges, i.e., in the $[1\bar{1}0]$ direction, leaves many of the $\times 1$ structural models, discussed in the previous subsection unchanged (see Fig. 2). Moreover, it turns out that the models listed in Table I again have the lowest surface energies. It seems that the Si(553)-Au surface prefers the symmetrical arrangement of the Au atoms in neighboring surface unit cells. The models with the asymmetrically arranged Au atoms in neighboring unit cells have much higher surface energies. What is also interesting, none of the most stable structural models leads to the buckling of the step edge Si atoms, in full agreement with the experimental results.[4–12] Thus one can assume that the model with the $\times 1$ periodicity (Fig. 1), i.e., the model with gold atoms in the positions Au_1 and Au_2, is a good candidate for a structural model of the Si(553)-Au surface. However, a more detailed inspection shows that this is not the case. It turns out, that in some of the $\times 2$ models, the Au atoms change their positions, leading to the dimerization of the Au atoms in the rows. This dimerization only slightly lowers the surface energy, like in the case of the models m2, m4, m7, and m8, or it leads to much larger changes in the energy, like in the case of the models m1, m9, and m10 (compare $\times 1$ and $\times 2$ models listed in Table I). The lowest energy $\times 2$ model (m1) is shown in Fig. 3. In this case, the dimerization of the Au atoms lowers the surface energy by 13.67 meV/Å^2, as compared to $\times 1$ m1 model. It is worthwhile to note that the local arrangement of the Au and Si_5 atoms is the same as in the recently proposed models of the Si(111)5$\times$2-Au reconstruction.[46–49] Moreover, the dimerization of the Au atoms leaves the structure at the step edges unchanged, i.e., no buckling of the step edges is observed, so the periodicity along the terraces still is equal to the Si-Si distance in the $[1\bar{1}0]$ direction. However, one can notice a sort of horizontal buckling, i.e., the Si_5 atoms alternate between left and right positions in the direction perpendicular to the steps (see Fig. 3), with distortion $\Delta y = 0.73$ Å. This fact is reflected in the STM topography and the band structure, as will be discussed in text sections.

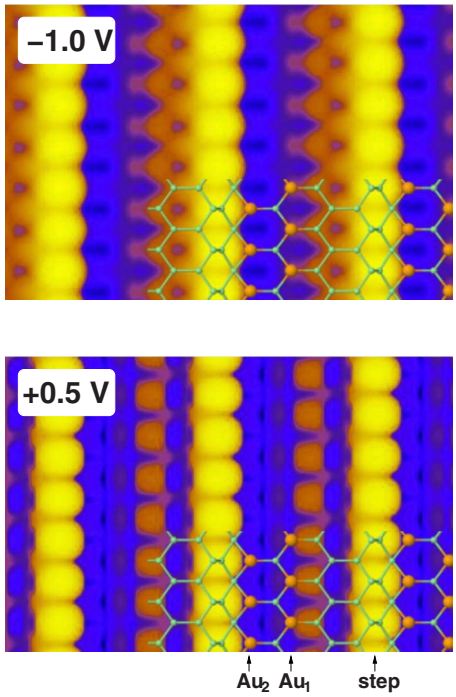

FIG. 4. (Color online) STM simulations of 4×2.6 nm^2 area of the Si(553)-Au surface, calculated for the m1 model with the $\times 1$ periodicity. Top (bottom) panel represents the filled (empty) state topography, respectively.

IV. STM TOPOGRAPHY

The STM topography data of the Si(553)-Au surface shows one-dimensional structures, which are interpreted as the step edge Si atoms.[4,18–20] Both structural models discussed in Sec. III support this scenario. To further check which one of two proposed models, i.e., $\times 1$ and $\times 2$ m1 models, is closer to a real model of the Si(553)-Au surface, the STM simulations within the Tersoff-Hamann approach[50] have been performed. The results of the filled and the empty state constant current topography calculated for the $\times 1$ and $\times 2$ m1 models are shown in Figs. 4 and 5, respectively.

Figure 4 represents the simulated STM topography of 4×2.6 nm^2 of the same area of the Si(553)-Au surface for sample bias $U = -1.0$ V (top panel) and $U = +0.5$ V (bottom panel), obtained within the $\times 1$ m1 model. As it was mentioned previously, the most visible chain structure is associated with the step edge Si atoms. The modulation of the topography along these chains is equal to the Si-Si distance in $[1\bar{1}0]$ direction, in agreement with STM experiments.[6,7,9,11,12] A less visible structure, observed at both polarizations, has been identified as due to the Si_4-Au_1 bonds (see Fig. 1). Similar structure, i.e., the chain with the $\times 1$ periodicity in the middle of terraces, has occasionally been observed in the STM experiments.[6,7,11]

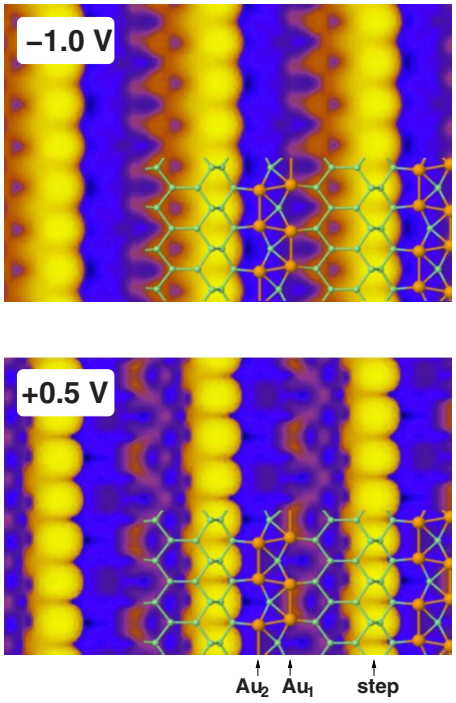

FIG. 5. (Color online) STM simulations of 4×2.6 nm^2 area of the filled (top) and the empty state (bottom) topography of the Si(553)-Au surface, calculated for the $\times2$ m1 model.

The corresponding simulated STM image generated from the $\times2$ m1 model of the Si(553)-Au surface is shown in Fig. 5. Top panel represents the filled state ($U=-1.0$ V), while the bottom one—the empty state topography ($U=+0.5$ V). Similar as in the $\times1$ m1 model (Fig. 4), the modulation of the topography along the step edge Si chain is equal to the $a_{[1\bar{1}0]}$. As one can notice, a less visible structure in the filled state image (top panel) coming from the bonding of the Si_4 and Au_1 atoms, is very similar to that obtained in the $\times1$ m1 model (see top panel of Fig. 4). However, due to the dimerization of the Au_1 atoms, the Si_4-Au_1 bonds are slightly rotated now, which is reflected in the STM image. On the other hand, the empty state topography (bottom panel of Fig. 5) is completely different from that of the $\times1$ m1 model. We observe a sort of zigzag structure now, which comes from the Au_1 dimers, Si_4 and Si_3 atoms (see Fig. 3). This could correspond to the experimentally observed similar structure.[6,7,9,11,12]

As we could see, both structural models, giving different topography images, seem to be consistent with the experimental results. So a question arises, how it is possible that we experimentally observe different topography images, once consistent with the $\times1$ m1 model, and another time, consistent with the $\times2$ m1 model. To be more precise, the STM topography recorded at the same conditions shows areas of different topographies. Some of the surface areas feature the structure in the middle of terraces with the $a_{[1\bar{1}0]}$ periodicity, and the other areas show the structures with double periodicity (see Fig. 1 of Ref. 6, Fig. 2 of Ref. 7, or Fig. 1 of Ref. 9). On the other hand, the chain structure associated with the step edge Si atoms always has the periodicity of the Si-Si distance in the direction $[1\bar{1}0]$. The most plausible scenario for such a behavior is that both structures are realized on real Si(553)-Au surface. The structure obtained within the single cell calculations appears to be a high-temperature phase, while the $\times2$ structure, with a lower energy, is a low temperature phase. At intermediate temperatures, both structures can be locally realized, as it is evident from the experimental data.[6,7,9] Moreover, the presence of defects, which could further stabilize one of the phases at intermediate temperatures, cannot be omitted. Nevertheless, at very low temperature, only the $\times2$ structure is expected to be observable.

V. BAND STRUCTURE

The experimentally measured electronic band structure features two one-dimensional bands (S_{12} and S_3) with parabolic dispersions.[4,5,7,13] Those bands cross the Fermi energy E_F at different $k_\parallel$, i.e., at 1.07 Å^{-1} (S_3 band), and around 1.27 Å^{-1} (S_{12} band).[7] The S_{12} band, crossing the E_F near the $\times2$ zone boundary ($k_\parallel=1.27$ Å^{-1} is split by 85 meV, and the splitting has its origin in the Rashba spin-orbit interaction.[13] Similar doublet of the proximal bands also is observed in the case of the Si(557)-Au surface,[27] and the bands are split due to the SO interaction.[28] It is expected that, also in the case of the Si(553)-Au surface, situation will be similar. Indeed, the DFT calculations for the f2 and p2* models of Ref. 20 (see Fig. 8 of Ref. 20), show that S_{12} band is spin split. However, the other features of the calculated band structure for those models disagree with the experimental data. In particular, in the case of the f2 model, the S_3 band also undergoes the SO splitting of the same magnitude as the S_{12} band. On the other hand, the agreement of the band structure calculated for the p2* model with the experimental data is slightly better, i.e., both bands (S_{12} and S_3) have similar dispersions but the SO splitting is stronger in the S_{12} band. However the band appearing at higher energies (S_3) also features some degree of splitting. Therefore it is natural to check the band structure calculated for the present ($\times1$ and $\times2$ m1) models against the ARPES data.[4,5,7,13] Although the SO interaction was not included in the present calculations, the main features of the band structure should be well reproduced.

Figure 6 shows the electronic band structure of the $\times1$ m1 model, calculated in the direction $[1\bar{1}0]$, i.e., parallel to the steps. The bands marked with open and the filled squares are those bands observed in photoemission experiments,[4,5,7] and come from the hybridization of the Au rows with the neighboring Si atoms. Both bands are metallic and cross the Fermi energy at $k_\parallel=1.18$ Å^{-1} (S_{12}) and 1.00 Å^{-1} (S_3), and slightly deviate from the experimentally determined values: 1.18–1.22 Å^{-1} and 1.04 Å^{-1} (Ref. 5) or 1.25–1.30 Å^{-1} and 1.07 Å^{-1}.[7] Moreover, bottom of the S_3 band (open squares) appears to be shifted toward the E_F by 0.4 eV with respect to the experimentally determined value of −0.64 eV.[4,5] The band marked with open circles, coming from the step edge Si atoms is not observed in photoemission, probably due to the zero amplitude of some matrix elements describing the photoemission process. However, there is also another possibility. In the case of the other vicinal Si surfaces, like the Si(557)-Au or the Si(335)-Au, this band is half occupied,[24,25]

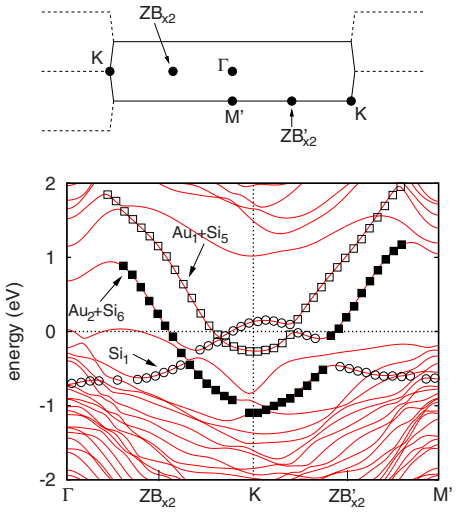

FIG. 6. (Color online) Top panel represents the two dimensional Brillouin zone for the $\times 1$ periodicity with the zone boundaries for the $\times 2$ structure ($ZB_{\times 2}$). The Γ-$ZB_{\times 2}$-K-$ZB'_{\times 2}$-M' direction is parallel to the steps of the Si(553)-Au surface. The band structure of the $\times 1$ m1 model is shown in the bottom panel. The atomic character of the bands is indicated by different symbols. Open (filled) squares mark the band coming from the hybridization of the Au_1 and Si_5 (Au_2 and Si_6) atoms (see Fig. 1), while the open circles stand for the step edge Si atoms band. The energies are measured from the Fermi energy (E_F=0).

and the periodicity doubling caused by the buckling of the step edge opens a gap in this band. As a result we have two bands: one fully occupied, and the other one—completely empty. Here, in the case of the Si(553)-Au surface, the situation is different. No buckling of the step edge was observed, however, due to the presence of additional row of Au atoms, this band becomes almost fully occupied. Perhaps in the real situation, this band can be further doped by some passivating atoms, and thus, shifted down in the energy. At the moment it is not clear why this band is not observed in the experiment, and the problem needs a further investigation.

The band structure calculated for the $\times 2$ m1 model, is shown in Fig. 7. Again, different symbols mark the different surface bands, similar as in Fig. 6. The open and the filled square bands are those bands observed in photoemission.[4,5,7] They have similar dispersions as in the case of the $\times 1$ m1 model, however the bands cross the Fermi energy at different $k_{\|}$ points, namely, at 1.22 Å^{-1} (S_{12}) and 1.03 Å^{-1} (S_3), which are closer to the experimental values, at least to those of Ref. 5. What is also important, energy of the bottom of the S_3 band coincides now with the experimentally determined value, i.e., −0.64 eV.[4,5] The band structure coming from the step edge Si atoms, marked as open circles, is now slightly more complicated. Namely, the periodicity doubling and the lateral buckling, discussed in Sec. III, open a gap in this

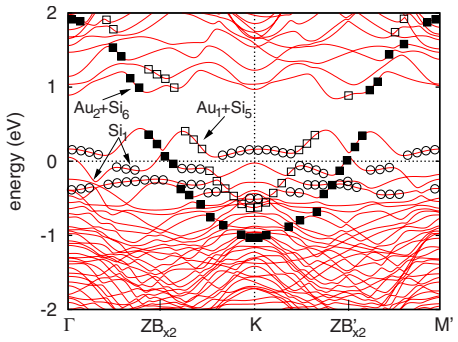

FIG. 7. (Color online) The band structure of the $\times 2$ m1 model, calculated in Γ-$ZB_{\times 2}$-K-$ZB'_{\times 2}$-M' direction of two-dimensional Brillouin zone shown in the top panel of Fig. 6. Again, the atomic character of the bands is indicated by different symbols, similar as in Fig. 6.

band. However, the step edge band again is almost fully occupied owing to the presence of the Au atoms.

As it was mentioned previously, the SO interaction was not included in the present calculations. Thus it is possible that the calculated band structures for the $\times 1$ and $\times 2$ m1 models may suffer from the same problem as the band structures of Ref. 20. Since both bands (S_{12} and S_3) have some contributions from gold, this may result in the SO splitting in both bands, not just in one as seen in the experiment.

All the above results show that the $\times 2$ m1 model is best candidate for a structural model of the Si(553)-Au surface, as this model is consistent with the STM and ARPES data and features the lowest surface energy. However, it is also possible that the $\times 1$ m1 model is locally realized on the Si(553)-Au surface.

VI. CONCLUSIONS

In conclusion, new structural model of the Au induced Si(553) surface has been proposed. The model accounts for experimentally found value of the Au coverage, i.e., 0.48 monolayer, which suggests the formation of two gold chains per Si(553) terrace. Such as the structural models of the other vicinal Si surfaces, the present model features the honeycomb chain. However, no buckling of the step edge is observed. The simulated STM topography images show the chain structure, associated with the step edge Si atoms. The calculated band structure features two metallic one-dimensional bands, coming from the hybridization of the Au atoms with the neighboring Si atoms. The experimentally determined band structure as well as the STM topography are well reproduced within the present model.

ACKNOWLEDGMENTS

I would like to thank M. Jałochowski for valuable discussions. This work has been supported by the Polish Ministry of Education and Science under Grant No. N N202 1468 33.

*krawiec@kft.umcs.lublin.pl

[1] M. Jałochowski, M. Stróżak, and R. Zdyb, Surf. Sci. **375**, 203 (1997).
[2] T. Giamarchi, *Quantum Physics in One Dimension* (Oxford University Press, New York, 2004).
[3] F. J. Himpsel, K. N. Altmann, R. Bennewitz, J. N. Crain, A. Kirakosian, J. L. Lin, and J. L. McChesney, J. Phys.: Condens. Matter **13**, 11097 (2001).
[4] J. N. Crain, J. L. McChesney, F. Zheng, M. C. Gallagher, P. C. Snijders, M. Bissen, C. Gundelach, S. C. Erwin, and F. J. Himpsel, Phys. Rev. B **69**, 125401 (2004).
[5] J. N. Crain, A. Kirakosian, K. N. Altmann, C. Bromberger, S. C. Erwin, J. L. McChesney, J.-L. Lin, and F. J. Himpsel, Phys. Rev. Lett. **90**, 176805 (2003).
[6] J. N. Crain and D. T. Pierce, Science **307**, 703 (2005).
[7] J. R. Ahn, P. G. Kang, K. D. Ryang, and H. W. Yeom, Phys. Rev. Lett. **95**, 196402 (2005).
[8] P. C. Snijders, S. Rogge, and H. H. Weitering, Phys. Rev. Lett. **96**, 076801 (2006).
[9] J. N. Crain, M. D. Stiles, J. A. Stroscio, and D. T. Pierce, Phys. Rev. Lett. **96**, 156801 (2006).
[10] J. N. Crain and F. J. Himpsel, Appl. Phys. A: Mater. Sci. Process. **82**, 431 (2006).
[11] K.-D. Ryang, P. G. Kang, H. W. Yeom, and S. Jeong, Phys. Rev. B **76**, 205325 (2007).
[12] P.-G. Kang, J. S. Shin, and H. W. Yeom, Surf. Sci. **603**, 2588 (2009).
[13] I. Barke, F. Zheng, T. K. Rügheimer, and F. J. Himpsel, Phys. Rev. Lett. **97**, 226405 (2006).
[14] I. Barke, R. Bennewitz, J. N. Crain, S. C. Erwin, A. Kirakosian, J. L. McChesney, and F. J. Himpsel, Solid State Commun. **142**, 617 (2007).
[15] S. K. Ghose, I. K. Robinson, P. A. Bennett, and F. J. Himpsel, Surf. Sci. **581**, 199 (2005).
[16] W. Voegeli, T. Takayama, K. Kubo, M. Abe, Y. Iwasawa, T. Shirasawa, T. Takahashi, K. Akimoto, H. Sugiyama, H. Tajiri, and O. Sakata, e-J. Surf. Sci. Nanotechnol. **6**, 281 (2008).
[17] T. Takayama, W. Voegli, T. Shirasawa, K. Kubo, M. Abe, T. Takahashi, K. Akimoto, and H. Sugiyama, e-J. Surf. Sci. Nanotechnol. **7**, 533 (2009).
[18] S. Riikonen and D. Sanchez-Portal, Nanotechnology **16**, S218 (2005).
[19] S. Riikonen and D. Sanchez-Portal, Surf. Sci. **600**, 1201 (2006).
[20] S. Riikonen and D. Sanchez-Portal, Phys. Rev. B **77**, 165418 (2008).
[21] M. Krawiec, T. Kwapiński, and M. Jałochowski, Phys. Status Solidi B **242**, 332 (2005).
[22] J. R. Ahn, H. W. Yeom, H. S. Yoon, and I. W. Lyo, Phys. Rev. Lett. **91**, 196403 (2003).
[23] M. Krawiec, T. Kwapiński, and M. Jałochowski, Phys. Rev. B **73**, 075415 (2006).
[24] S. Riikonen and D. Sanchez-Portal, Phys. Rev. B **76**, 035410 (2007).
[25] M. Krawiec, Phys. Rev. B **79**, 155438 (2009).
[26] Differences in $k_{\|}$ at which bands cross the Fermi energy come from uncertainty in determination of the E_F due to photovoltaic effect.
[27] R. Losio, K. N. Altmann, A. Kirakosian, J.-L. Lin, D. Y. Petrovykh, and F. J. Himpsel, Phys. Rev. Lett. **86**, 4632 (2001).
[28] D. Sanchez-Portal, S. Riikonen, and R. M. Martin, Phys. Rev. Lett. **93**, 146803 (2004).
[29] M. Krawiec, Appl. Surf. Sci. **254**, 4318 (2008).
[30] I. Barke, F. Zheng, S. Bockenhauer, K. Sell, V. v. Oeynhausen, K. H. Meiwes-Broer, S. C. Erwin, and F. J. Himpsel, Phys. Rev. B **79**, 155301 (2009).
[31] W. Swiech, E. Bauer, and M. Mundschau, Surf. Sci. **253**, 283 (1991).
[32] E. Bauer, Surf. Sci. Lett. **250**, L379 (1991).
[33] P. Ordejon, E. Artacho, and J. M. Soler, Phys. Rev. B **53**, R10441 (1996).
[34] D. Sanchez-Portal, P. Ordejon, E. Artacho, and J. M. Soler, Int. J. Quantum Chem. **65**, 453 (1997).
[35] E. Artacho, D. Sanchez-Portal, P. Ordejon, A. Garcia, and J. M. Soler, Phys. Status Solidi B **215**, 809 (1999).
[36] J. M. Soler, E. Artacho, J. D. Gale, A. Garcia, J. Junquera, P. Ordejon, and D. Sanchez-Portal, J. Phys.: Condens. Matter **14**, 2745 (2002).
[37] E. Artacho, E. Anglada, O. Dieguez, J. D. Gale, A. Garcia, J. Junquera, R. M. Martin, P. Ordejon, J. M. Pruneda, D. Sanchez-Portal, and J. M. Soler, J. Phys.: Condens. Matter **20**, 064208 (2008).
[38] J. P. Perdew and A. Zunger, Phys. Rev. B **23**, 5048 (1981).
[39] N. Troullier and J. L. Martins, Phys. Rev. B **43**, 1993 (1991).
[40] F. C. Chuang, C. V. Ciobanu, C. Predescu, C. Z. Wang, and K. M. Ho, Surf. Sci. **578**, 183 (2005).
[41] F. C. Chuang, C. V. Ciobanu, C. Z. Wang, and K. M. Ho, J. Appl. Phys. **98**, 073507 (2005).
[42] R. M. Briggs and C. V. Ciobanu, Phys. Rev. B **75**, 195415 (2007).
[43] C. V. Ciobanu, F. C. Chuang, and D. E. Lytle, Appl. Phys. Lett. **91**, 171909 (2007).
[44] The Au chemical potential $\mu_{\mathrm{Au}}^{\mathrm{bulk}}$ is taken as the calculated energy per gold atom in the bulk.
[45] S. C. Erwin and H. H. Weitering, Phys. Rev. Lett. **81**, 2296 (1998).
[46] S. Riikonen and D. Sanchez-Portal, Phys. Rev. B **71**, 235423 (2005).
[47] C.-Y. Ren, S.-F. Tsay, and F.-C. Chuang, Phys. Rev. B **76**, 075414 (2007).
[48] A. Stępniak, P. Nita, M. Krawiec, and M. Jałochowski, Phys. Rev. B **80**, 125430 (2009).
[49] S. C. Erwin, I. Barke, and F. J. Himpsel, Phys. Rev. B **80**, 155409 (2009).
[50] J. Tersoff and D. R. Hamann, Phys. Rev. Lett. **50**, 1998 (1983); Phys. Rev. B **31**, 805 (1985).